

Cite this: *J. Mater. Chem. A*, 2017, 5, 11450

## Mixed cation hybrid lead halide perovskites with enhanced performance and stability

Feng Xu, Taiyang Zhang, Ge Li and Yixin Zhao \*

Organic and inorganic hybrid perovskites have emerged as revolutionary optoelectronic semiconductors, which are promising for various applications especially in photovoltaics and light-emitting diodes. Perovskite solar cells have demonstrated unprecedented progress on PCE within a very short time in the history of photovoltaics. Perovskite solar cells have more than 20% PCE and advantages such as easy-to-process and tunable bandgaps have made them favorable for commercialization. Extending the absorption to a longer wavelength and addressing the challenge of stability in metal halide perovskites has become the most important research focus. However, composition engineering could be a potential solution by further tuning the band gap for the metal halide perovskites and, thus, enhance their stability. The mixed cation perovskite is one of the most practical and successful strategies for composition engineering. Here, recent progress on mixed cation metal halide perovskites is reviewed and this includes the development of binary, ternary and two-dimensional/three-dimensional mixed cation perovskites in chemical synthesis and device performance and stability progress. The prospects and challenges for the mixed cation hybrid perovskites are also considered.

Received 3rd January 2017  
Accepted 17th March 2017

DOI: 10.1039/c7ta00042a

rsc.li/materials-a

### Introduction

The past few years have witnessed the increase of interest of perovskite solar cells (PSCs) with a certified solar cell PCE of 22.1%<sup>1</sup> and a module PCE of 12% for 6 × 6 cm<sup>2</sup> size cells. Such

*School of Environmental Science and Engineering, Shanghai Jiao Tong University, 800 Dongchuan Road, Shanghai 200240, China. E-mail: yixin.zhao@sjtu.edu.cn*



*Professor Yixin Zhao received his BS and MS degrees in Chemistry from the Shanghai Jiao Tong University in China in 2002 and 2005, respectively. He obtained his Ph.D. from Case Western Reserve University in 2010, and then he worked as postdoctoral fellow at the Pennsylvania State University and National Renewable Energy Laboratory. His current research interests focus on functional materials for*

*renewable energy and environmental remediation including perovskite solar cells, water splitting and photocatalysis. Dr Zhao has published more than 70 peer-reviewed papers in Chem. Rev., Chem. Soc. Rev., PNAS, Nat. Commun., J. Am. Chem. Soc., Angew. Chem. Int. Ed., Energy Environ. Sci., Adv. Mater., Nano Lett. and many more.*

a performance level is comparable to that obtained with commercial silicon solar cells. This is the first time a third generation solar cell technology has demonstrated the potential for commercialization with such great promise in such a short time. The progress has made organic–inorganic hybrid halide perovskites become one of the most intensively studied research topics by researchers in many different disciplines.<sup>2–5</sup> The most typical organic–inorganic perovskite is methylammonium triiodoplumbate (CH<sub>3</sub>NH<sub>3</sub>PbI<sub>3</sub>; MAPbI<sub>3</sub>), which had been synthesized and characterized in the early 1980s.<sup>6,7</sup> The MAPbI<sub>3</sub> was used for the first time in 2009 as a light absorber by Kojima *et al.* and was used in a typical dye-sensitized solar cell (DSSC) device using liquid electrolyte with less than 4% PCE.<sup>8</sup> Park *et al.* later pushed the PCE of liquid electrolyte perovskite-sensitized solar cells to ~6%, but this performance was still lower than that of the conventional DSSC.<sup>8,9</sup> Although this pioneering work did not show promising performance at that time, the biggest issue related to use of MAPbI<sub>3</sub> was identified, which is the poor stability of the liquid electrolyte. The issue of liquid electrolyte was soon solved by using solid-state electrolytes. In 2012, reports of several breakthrough demonstrated that the solid-state MAPbI<sub>3</sub> PSCs exhibited 10–11% photoelectron conversion with much better stability.<sup>10–12</sup> Such PCE is much higher than that obtained with the solid-state DSSCs and is comparable to the state-of-the-art polymer solar cells. Since then, the MAPbI<sub>3</sub> based PSCs have progressed in terms of their PCE after the tremendous research efforts on perovskite film deposition and interface engineering.<sup>13–17</sup>

These significant developments especially the progress made in the PCE of MAPbI<sub>3</sub> perovskite solar cells introduce the importance of the stability issue. The most obvious challenge to stability of lead halide perovskites is their sensitivity to moisture and polar solvents. The moisture sensitivity can be solved by using sealing techniques and some other surface passivation techniques such as atomic layer deposition.<sup>18</sup> However, the intrinsic high temperature phase instability of MAPbI<sub>3</sub> perovskite became the main obstacle to further development of perovskite for reliable photovoltaic (PV) or other optoelectronic applications. Besides the stability issue, the band gap of MAPbI<sub>3</sub> perovskite is around 1.55 eV, which is not ideal for solar cells. To overcome the issue of high temperature phase instability and electronic structure existing in the MAPbI<sub>3</sub> perovskite, composition optimization became a promising approach to enhance the phase stability and modify the electronic structure. For the ABX<sub>3</sub> halide perovskite, the cation, halide and metal composition can all be tuned to modify the properties of the final perovskite. Among them, the mixed cation perovskite exhibited the most promising potential to enhance both the PCE and stability. In this review, the latest progress and trend of mixed cation organic–inorganic hybrid lead halide perovskites will be focused on and there is a brief consideration on the challenges and opportunities of mixed cation lead halide perovskites with enhanced performance and stability.

## Binary cation perovskite

### FA–MA mixed cation perovskite

Although cations in the A site have no direct contribution to band structure in the perovskite structure ABX<sub>3</sub>, cations of different sizes can expand or contract the lattice of the whole structure and change the B–X bond length resulting in a different band gap.<sup>19,20</sup> Currently, the most widely used cations to form a perovskite structure with lead halide are CH<sub>3</sub>NH<sub>3</sub><sup>+</sup> (MA<sup>+</sup>), HC(NH<sub>2</sub>)<sub>2</sub><sup>+</sup> (FA<sup>+</sup>) and Cs<sup>+</sup>. FA accounts for a broader absorption in formamidinium lead iodide (FAPbI<sub>3</sub>) as it expands the lattice of perovskite structure ABX<sub>3</sub> because of its larger size than MA. Thus, substitution of MA with FA has been an attractive way to tune the band gap of MAPbI<sub>3</sub> and lead to a redshift of optical absorbance. However, it is difficult to obtain high quality  $\alpha$ -FAPbI<sub>3</sub> because the FAPbI<sub>3</sub> has a tolerance factor larger than 1,<sup>20</sup> which requires a higher crystallization temperature and results in the easy-to-form, unwanted yellow phase.

### Sequential deposition

The binary cation perovskite of MA<sub>x</sub>FA<sub>1-x</sub>PbI<sub>3</sub> was reported by Grätzel group for the first time.<sup>21</sup> To obtain a high quality and smooth perovskite film, this mixed perovskite (MA)<sub>x</sub>(FA)<sub>1-x</sub>PbI<sub>3</sub> was prepared *via* a sequential deposition method by dipping lead iodide (PbI<sub>2</sub>) in methylammonium (MAI) + formamidinium iodide (FAI) mixed solution (Fig. 1a). In this work, the characteristic diffraction peaks at 14.0°, 28.4°, and 31.8° in X-ray diffraction (XRD) patterns decrease with the addition of FA as well as an onset of redshift in the ultraviolet-visible (UV-vis) absorbance. There are some impurity peaks of MAPbI<sub>3</sub> and  $\delta$ -

FAPbI<sub>3</sub> in their XRD patterns, which reveal the difficulty of obtaining the phase-pure mixed cation (MA)<sub>x</sub>(FA)<sub>1-x</sub>PbI<sub>3</sub> perovskites *via* regular sequential deposition. The PCE of such a mixed cation perovskite was comparable to that of MAPbI<sub>3</sub> based solar cells at that time. Because the short-circuit current density ( $J_{sc}$ ) is relatively low in the fully printable, hole conductor free, mesoscopic MAPbI<sub>3</sub> solar cells of Hu *et al.*, they tried using a FA and MA mixed cation perovskite with a FAI/MAI molar ratio of 3/2 as light absorber using a sequential deposition method to achieve a PCE of 12.9%, which was higher than that obtained with pure MAPbI<sub>3</sub> or FAPbI<sub>3</sub>.<sup>22</sup> The increasing PCE was attributed to the fact that the absorption onset of the perovskite shifted to longer wavelengths to improve the incident photoelectron conversion (IPCE) in the spectral range from 660 nm to 750 nm. Because the determinative intercalation kinetic of FA and MA cations might be different, it was difficult to control the FA and MA ratio in the final films using a traditional sequential deposition method. To control the FA content in the final films, Liu *et al.* developed a novel strategy to obtain a non-stoichiometric (FAI)<sub>1-x</sub>-PbI<sub>2</sub> intermediate complex firstly as a precursor for sequential deposition using the MAI solution instead of the MAI + FAI mixture solution.<sup>23</sup> In this method as shown in Fig. 1b, the larger size FA is firstly intercalated and fixed into the PbI<sub>2</sub> crystal lattice. Then the MAI is later intercalated into the precursor film to form the phase pure MA<sub>x</sub>FA<sub>1-x</sub>PbI<sub>3</sub>. With this method, the MA/FA ratio can be controlled more precisely without forming the impure phase. The best device based on MA<sub>0.6</sub>FA<sub>0.4</sub>PbI<sub>3</sub> using this method showed a higher photocurrent and broader IPCE spectrum than that obtained with MAPbI<sub>3</sub> with a power conversion efficiency (PCE) of over 13%.

The excellent PV properties of the mixed MA<sub>x</sub>FA<sub>1-x</sub>PbI<sub>3</sub> perovskite have attracted many researchers to the fundamental investigations and thus, develop mixed cation perovskites. Dai *et al.* prepared mixed MA<sub>x</sub>FA<sub>1-x</sub>PbI<sub>3</sub> nanorods stabilized within the perovskite structure while the photoluminescence (PL) emission was shifted from 821 nm to 782 nm as the MA ratio ( $x$ ) increased from 0 to 1. The mixed cation MA<sub>x</sub>FA<sub>1-x</sub>PbI<sub>3</sub> nanorods also had a longer PL lifetime than the pure FAPbI<sub>3</sub> or MAPbI<sub>3</sub> nanorods.<sup>24</sup> Because the diffusion coefficient in the MAPbI<sub>3</sub> perovskite is larger than that in the FAPbI<sub>3</sub> perovskite, mixing FA with MA was found to balance the PV property and the stability of the cell devices.<sup>25</sup> The incorporation of a small amount of MA (15%) into FAPbI<sub>3</sub> helped with the stable formation of trigonal FAPbI<sub>3</sub> without the requirement of a high annealing temperature and there was no lattice shrinkage or optical changes.<sup>26</sup> The incorporation of MA significantly enhanced the stability of the PbI<sub>6</sub> octahedral three-dimensional (3D) structure because of the I–H bond between the cation and the inorganic PbI<sub>6</sub>, in which the MA exhibits a dipole moment 10 times larger than that of FA (Fig. 2).

In the previously mentioned two-step or sequential deposition method, the precursor is either PbI<sub>2</sub> or a PbI<sub>2</sub>-based precursor film with partial FAI intercalation followed by further interaction with MAI and/or FAI. In these methods, the interaction process includes the intercalation of both cation and halide ions. Later the cation only exchange method was developed. Because the high quality MAPbI<sub>3</sub> can be easily deposited

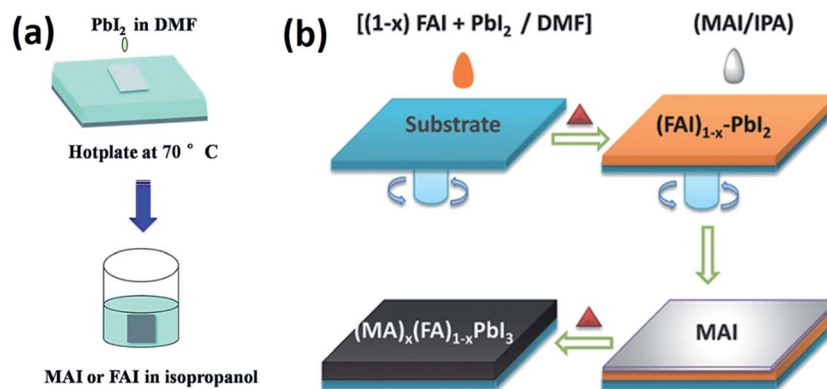


Fig. 1 Schematic illustration of (a) the sequential deposition method. Reproduced from ref. 22 with permission from the Royal Society of Chemistry. (b) Preparation of phase-pure  $\text{MA}_x\text{FA}_{1-x}\text{PbI}_3$  perovskites via first forming  $(\text{FAI})_{1-x}\text{-PbI}_2$  followed by intercalation of MAI. Reprinted with permission from ref. 23. Copyright© 2015 WILEY-VCH Verlag GmbH & Co. KGaA, Weinheim.

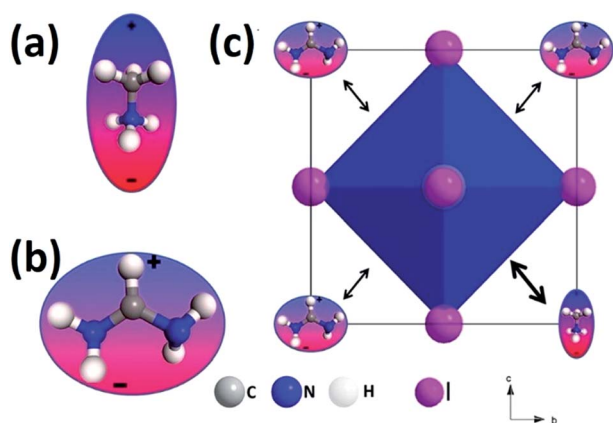


Fig. 2 (a) and (b) Schematic illustration of the MA and FA cation, respectively. (c) Different effect of the cations on the perovskite structure. Reprinted with permission from ref. 26. Copyright 2015 American Chemical Society.

with various perovskite deposition techniques, these cation exchange methods usually adopted a high quality  $\text{MAPbI}_3$  film as the precursor film. As shown in Fig. 3a, the FA/MA mixed cation perovskite was fabricated by dipping  $\text{MAPbI}_3$  film into FAI solution with an increase of the dipping temperature to  $60^\circ\text{C}$  to promote the FA exchange in  $\text{MAPbI}_3$ .<sup>27</sup> The dipping time was shortened and the undesirable phase transition was restricted at temperatures under  $60^\circ\text{C}$ . The inter-conversion between  $\text{MAPbI}_3$  and  $\text{FAPbI}_3$  was demonstrated via a cation exchange reaction involving dipping the  $\text{MAPbI}_3$  (or  $\text{FAPbI}_3$ ) films in a solution of  $10\text{ mg ml}^{-1}$  FAI (or MAI) in propan-2-ol at room temperature, which allowed bandgap tuning between 1.57 and 1.48 eV.<sup>28</sup> A mixed cation perovskite of  $(\text{MA}_x\text{FA}_{1-x}\text{PbI}_3)$  made using this incomplete inter-conversion shows improved solar cell performances and phase stability. Besides these traditional sequential deposition methods in solution chemistry to obtain the MA/FA mixed cation perovskites, Zhou *et al.* also demonstrated a gas/solid method to induce the cation exchange reaction to convert the as-synthesized high quality  $\text{MAPbI}_3$  perovskite thin films into  $\text{FA}_x\text{MA}_{1-x}\text{PbI}_3$  by introducing

the  $\text{MAPbI}_3$  film in FA gas at  $150^\circ\text{C}$  [Fig. 3(b)]. Similar to the ion-exchange process in all the sequential deposition methods, the alloy content for the final product can be controlled by using different cation exchange reaction times.<sup>29</sup>

### One-step method

Although the high quality MA/FA mixed cation perovskites can be prepared successfully via cation intercalation or a cation exchange reaction in the sequential deposition methods, the precise control of the MA/FA ratio and avoiding the gradient of the MA/FA ratio are still challenging because of the intrinsic limitation of these methods. However, the precise MA/FA ratio in the precursor solutions can be controlled in the one-step method. Manuel *et al.* studied mixed cation perovskite  $\text{MA}_x\text{-FA}_{1-x}\text{PbI}_3$  (where  $x = 0-1$ ) for solar cell fabrication using a one-step solvent engineering method.<sup>30</sup> The best PCE was achieved in the mixed cation perovskite  $\text{MA}_{0.6}\text{FA}_{0.4}\text{PbI}_3$  solar cells. The low addition of FAI from 15% to 40% can also reduce the hysteresis behavior. It was revealed that the FA cation alloying slows down the crystal formation in perovskites resulting in larger crystals and a high degree of order.<sup>30</sup> Although the content of  $\text{FAPbI}_3$  used gives a higher stability as well as higher performance than  $\text{MAPbI}_3$ , the high annealing temperature required makes it difficult to obtain high quality films.

To further enhance the performance and stability of the FA/MA mixed cation perovskite, bromine (Br) can also be introduced to partially replace the iodine (I) in the perovskite. The incorporation of a small amount of  $\text{MABr}$  into  $\text{FAPbI}_3$  was also found to help relax the anisotropic strained lattice and stabilizes the perovskite phase.<sup>31-33</sup> Jeon *et al.* and Kim *et al.* developed a classic composite recipe of  $(\text{FAPbI}_3)_{0.85}(\text{MAPbBr}_3)_{0.15}$  for fabrication of FA/MA mixed cation perovskite films with a superior PCE via a one-step method.<sup>34,35</sup> Various compositions with different FA/MA and I/Br ratios have also been tried since.<sup>36-38</sup> Jacobsson *et al.* systematically explored the MA/FA-Pb-I/Br perovskite by gradually replacing iodide and MA with bromide and FA with 49 different ratios of MA/FA and I/Br in the perovskite and then performing material characterization and device fabrication with them.  $\text{MA}_{2/6}\text{FA}_{4/6}\text{Pb}(\text{Br}_{1/6}\text{I}_{5/6})_3$  was outstanding

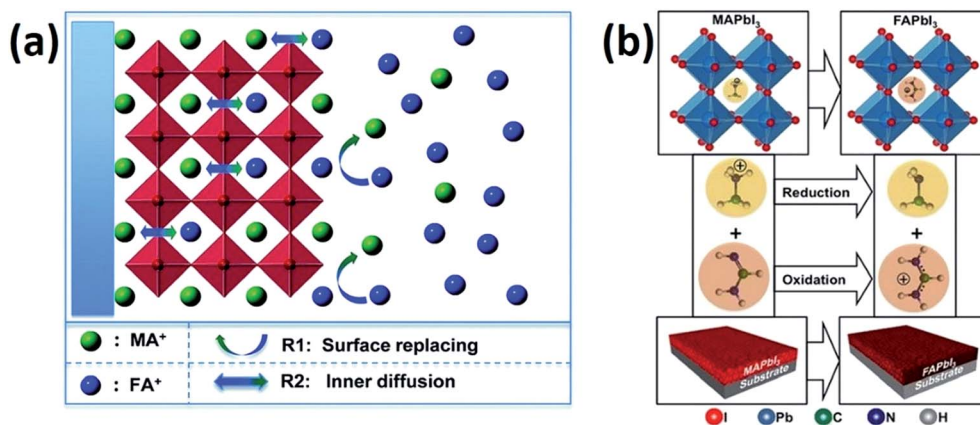


Fig. 3 Schematic illustration of (a) cation exchange between the MAPbI<sub>3</sub> precursor film and FAI solution to obtain FAPbI<sub>3</sub> film. Reproduced from ref. 27 with permission from the Royal Society of Chemistry. (b) Cation exchange between the MAPbI<sub>3</sub> precursor film and FA gas at 150 °C to obtain FAPbI<sub>3</sub> film. Reprinted with permission from ref. 29. Copyright 2016 American Chemical Society.

among all the perovskites that were compared and the best PCE obtained was 20.67%.<sup>39</sup> A heterogeneous crystalline structure shown as nanoscale segregation and “inverted” hysteresis were also found in the mixed (FAPbI<sub>3</sub>)<sub>1-x</sub>(MAPbBr<sub>3</sub>)<sub>x</sub> perovskite.<sup>40,41</sup> With the outstanding PV properties of mixed (FAPbI<sub>3</sub>)<sub>1-x</sub>(MAPbBr<sub>3</sub>)<sub>x</sub> perovskite, this mixed cation perovskite has become a model perovskite layer used in various studies of electron transport layer, hole transport materials and device structures.<sup>42-54</sup> Other than Br, Isikgor *et al.* also introduced chloride (Cl) into a FA/MA mixed cation perovskite to form the MA<sub>1-x</sub>FA<sub>x</sub>PbI<sub>3-y</sub>Cl<sub>y</sub> mixed perovskite. The optimal PCE was 18.14% for the planar PSCs with MA<sub>0.20</sub>FA<sub>0.80</sub>PbI<sub>3-y</sub>Cl<sub>y</sub>, significantly outperforming the PSCs with other perovskite compositions including MAPbI<sub>3</sub>, MAPbI<sub>3-y</sub>Cl<sub>y</sub>, MAPbI<sub>3-y</sub>Cl<sub>y</sub>, and MA<sub>1-x</sub>FA<sub>x</sub>PbI<sub>3</sub>.<sup>55</sup> The solvent engineering method is the most popular one-step method used to prepare the FA/MA mixed cation perovskite because in the other popular one-step methods such as the additive method, the introduction of some extra cations might affect the final FA/MA ratio in the final perovskite films. Recently, a two-dimensional (2D)-3D conversion strategy was developed to obtain a high quality phase-pure 3D MA<sub>1-x</sub>FA<sub>x</sub>PbI<sub>3</sub> ( $x = 0.1-0.9$ ) perovskites using a simple one-step method. In this method, a compact 2D mixed composition HMA<sub>1-x</sub>FA<sub>x</sub>PbI<sub>3</sub>Cl perovskite

precursor film was designed to fabricate MA<sub>1-x</sub>FA<sub>x</sub>PbI<sub>3</sub>. The thermodynamically preferred Cl/I and H/FA(MA) ion exchange reaction induced fast transformation of 2D HMA<sub>1-x</sub>FA<sub>x</sub>PbI<sub>3</sub>Cl perovskite film into phase-pure and high quality MA<sub>1-x</sub>FA<sub>x</sub>PbI<sub>3</sub> with complete removal of HCl (Fig. 4).<sup>56</sup>

Other than the high PCE obtained using the FA/MA mixed cation perovskite solar cells,  $a > 1000$  h outdoor stability was demonstrated in the mixed cation perovskite with a configuration of fluorine doped tin oxide/titanium dioxide (TiO<sub>2</sub>)/(FAPbI<sub>3</sub>)<sub>0.85</sub>(MAPbBr<sub>3</sub>)<sub>0.15</sub>/Spiro-OMeTAD/gold (Au).<sup>57</sup> The PSCs maintained 80% of their initial PV properties after 846 h under continuous outdoor atmospheric analyses. Based on previous studies of preparing perovskite in ambient air, the fabrication of mixed (FAPbI<sub>3</sub>)<sub>1-x</sub>(MAPbBr<sub>3</sub>)<sub>x</sub> perovskite solar cells can be processed under an ambient atmosphere and maintain an excellent performance.<sup>58</sup> This progress demonstrates the promising potential of better stability based on the MA/FA mixed cation perovskite.

#### FA/MA-Cs mixed cation perovskite

Another big issue for the organic hybrid halide perovskites is degradation because of the volatility of the organic cations.<sup>59,60</sup> As a result of this, an all-inorganic perovskite, CsPbX<sub>3</sub> has been become another research focus recently. The  $\alpha$ -cesium lead iodide ( $\alpha$ -CsPbI<sub>3</sub>) has a suitable band gap of 1.7 eV for PV applications. Unfortunately,  $\alpha$ -CsPbI<sub>3</sub> film formation requires a high annealing temperature of over 300 °C. Eperon *et al.* found that a small addition of hydroiodic acid into the regular CsPbI<sub>3</sub> precursor solution as an additive could help form smooth thin CsPbI<sub>3</sub> films at a low temperature of 100 °C.<sup>60</sup> However, the low PCE and the instability of the desired black phase place it at a disadvantage compared against all-organic perovskites. The low stability of  $\alpha$ -CsPbI<sub>3</sub> can be ascribed to its very low tolerance factor because the Goldschmidt tolerance factor ( $t$ ) is an important index for a cubic perovskite structure controlled between 0.8 and 1.0 by tuning the ionic radius in the composition (Fig. 5b).<sup>61</sup> The tolerance factor of CsPbI<sub>3</sub> is out of 0.8-1.0 range, which also accounts for its low phase stability at room temperature. To tune

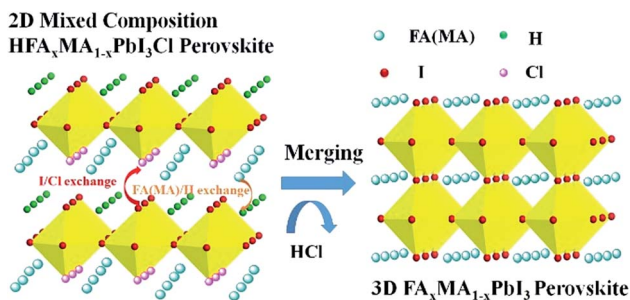


Fig. 4 Schematic of formation of 3D MA<sub>1-x</sub>FA<sub>x</sub>PbI<sub>3</sub> from 2D mixed composition A<sub>2</sub>BX<sub>4</sub> of HMA<sub>1-x</sub>FA<sub>x</sub>PbI<sub>3</sub>Cl (A = H, MA, FA, B = Pb, X = I, Cl). Reprinted with permission from ref. 56. Copyright© 2016 Wiley-VCH Verlag GmbH & Co. KGaA, Weinheim.

the  $t$  to a suitable range, the mixed halide  $\text{CsPbBr}_x\text{I}_{3-x}$  (with  $0.6 < x < 1.2$ ) perovskite can be phase stable with improved PV performance.<sup>62</sup> Unfortunately, the incorporation of Br widens the band gap of  $\text{CsPbI}_3$ , which is undesired for PV applications. To realize better PV performance for  $\text{CsPbI}_3$  and less volatile composition in the hybrid lead halide perovskite, a Cs-based mixed cation perovskite containing MA or FA has been reported because both FA- and MA-based perovskite have a larger tolerance factor to tune the Cs-based perovskite. Li *et al.* have demonstrated a  $\alpha$ - $\text{Cs}_x\text{FA}_{1-x}\text{PbI}_3$  fabricated using a regular one-step solvent engineering method with different Cs/FA ratios. The best  $\text{FA}_{0.85}\text{Cs}_{0.15}\text{PbI}_3$  film showed humidity resistance without  $\alpha$ -to- $\delta_{\text{H}}$  phase transition and can be stabilized as  $\alpha$ -phase at room temperature.<sup>61</sup> This phase-pure  $\alpha$ - $\text{Cs}_x\text{FA}_{1-x}\text{PbI}_3$  perovskite can be attained at an annealing temperature lower than 150 °C and 315 °C for  $\alpha$ -FAPbI<sub>3</sub> and  $\alpha$ -CsPbI<sub>3</sub>, respectively. Lee *et al.* demonstrated that the  $\text{FA}_{0.9}\text{Cs}_{0.1}\text{PbI}_3$  perovskite exhibited both better stability and PCE for solar cells than the pure FAPbI<sub>3</sub> perovskite.<sup>63</sup> In this work, lead(II) iodide ( $\text{PbI}_2$ ), FAI and cesium iodide (CsI) were dissolved in dimethylformamide (DMF) and dimethylsulfoxide (DMSO) was added as a co-solvent to form a so-called intermediate phase  $\text{FA}(\text{Cs})\text{I}-\text{PbI}_2$ -DMSO and the best PCE performance of 16.5% was achieved.

Furthermore, the effect of cation mixing in Cs and FA mixed hybrid halide perovskites was elucidated *via* theoretical and experimental investigations.<sup>64,65</sup> Yi *et al.* discovered that the best

PCE was improved up to 18% by replacing both a small fraction of the iodide and bromide anions as  $\text{Cs}_{0.2}\text{FA}_{0.8}\text{PbI}_{2.84}\text{Br}_{0.16}$ , which is similar to the FA/MA mixed perovskite with incorporation of some Br to improve the performance.<sup>64</sup> These perovskite films were also fabricated *via* a one-step anti-solvent method. In the mixed Cs-FA perovskite, the dark  $\alpha$ -phase forms at room temperature when anti-solvent chlorobenzene was added during spin coating without reversible phase transition to the yellow  $\delta$ -phase. The stable perovskite rather than the non-perovskite resulting from the structural and unit volume difference of  $\delta$ - $\text{CsPbI}_3$  and  $\delta$ -FAPbI<sub>3</sub> and the similarity of the  $\alpha$ - and  $\beta$ -phases for  $\text{CsPbI}_3$  and FAPbI<sub>3</sub> is shown in Fig. 5a. In this case, mixing the  $\alpha$ - or  $\beta$ -phases for  $\text{CsPbI}_3$  and FAPbI<sub>3</sub> is more favorable than using the  $\delta$ -phase for the lower energetic contribution of mixing. McMeekin *et al.* also reported a FA/Cs mixed cation perovskite of  $\text{FA}_{0.83}\text{Cs}_{0.17}\text{PbI}_3$  with some added bromide to achieve a band gap of 1.75 eV.<sup>66</sup> Finally, this  $\text{FA}_{0.83}\text{Cs}_{0.17}\text{Pb}(\text{I}_{0.6}\text{Br}_{0.4})_3$  perovskite solar cell realized an open-circuit voltage reaching 1.2 V with a PCE of over 17%. The mixed perovskite of  $\text{FA}_{0.83}\text{Cs}_{0.17}\text{Pb}(\text{I}_{0.6}\text{Br}_{0.4})_3$  as the absorber layer was utilized in the newly designed n-i-p planar heterojunction perovskite device with an n-doped  $\text{C}_{60}$  charge collection layer.<sup>67</sup> After 650 h under ambient air without encapsulation and over 3400 h with encapsulation, 80% of the original PCE was sustained. Beside the FA, the MA cation has also been alloyed with Cs to form the MA/Cs mixed perovskites.

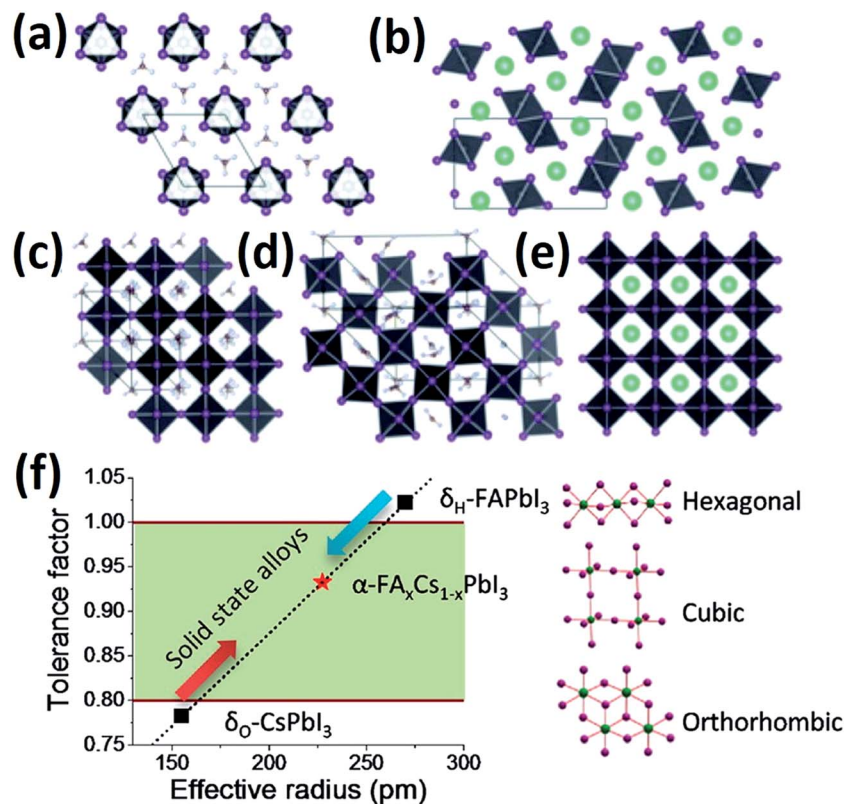


Fig. 5 (a) and (b) The  $\delta$ -phase of FA and Cs perovskites. (c) and (d) The  $\alpha$ - and  $\beta$ -phases of FAPbI<sub>3</sub>. (e) The cubic phase of CsPbI<sub>3</sub>. Reproduced from ref. 64 with permission from the Royal Society of Chemistry. (f) Relationship of the Goldschmidt tolerance factor ( $t$ ) and radius of atoms. Reprinted with permission from ref. 61. Copyright 2016 American Chemical Society.

Original Cs containing MA perovskite solar cells with inverted type planar heterojunction PSCs were developed by Choi *et al.* using [6,6]-phenyl-C<sub>60</sub> butyric acid methyl ester as an electron acceptor.<sup>68</sup> Use of 10% Cs doping in MAPbI<sub>3</sub> perovskite improved the PCE from 5.51% to 7.68%.

### Ternary cation perovskite

The previously mentioned binary cation perovskites all exhibited improved performance and stability. Therefore, a ternary cation perovskite using MA, FA and Cs perovskite was also successfully developed. The first FA, MA and Cs triple cation perovskite was reported by Saliba *et al.* and it was found that using Cs can improve the film quality for the FA/MA mixture.<sup>69</sup> CsI (5%) was incorporated into the (FAPbI<sub>3</sub>)<sub>0.83</sub>(MAPbBr<sub>3</sub>)<sub>0.17</sub> mixed cation perovskite to suppress the non-perovskite phase and enhance the crystallization process. As shown in Fig. 6a, a highly stabilized PCE at 21.1% was achieved and the cells still maintained a PCE of 18% after 250 h. Matsui *et al.* also optimized the MA/Cs ratio with a fixed I/Br ratio of 0.83/0.17 and a FA ratio of 0.8.<sup>70</sup> The “complex-assisted gas quenching” method was also used to deposit pinhole free triple cation Cs/MA/FA perovskite.<sup>71</sup> In this method, DMSO was used to form a DMSO–PbX<sub>2</sub> complex and it is a widely used method to fabricate different types of perovskite materials. It has been thought that only a few monovalent cations can meet the conditions stated previously, including MA, FA and Cs, including a suitable Goldschmidt tolerance factor for the perovskite crystal structure between 0.8 and 1.0.<sup>72,73</sup> Very recently, Saliba *et al.* investigated several alkali cations and found that the radius of rubidium (Rb) was only slightly smaller than the favorable cations of Cs, MA and FA. They successfully alloyed a small amount of rubidium iodide (RbI; about 5% to 10%) into a Cs/MA/FA mixed cation perovskite to achieve a record PCE of 21.6% on small areas and 19.0% on large areas (0.5 cm<sup>2</sup>) under AM1.5G. Because the entropy of the mixed compounds increases, the addition of Rb suppresses the formation of the unwanted yellow phase of Cs or FA perovskite and improves the stability of solar cells. The device based on Rb/Cs/MA/FA perovskite could maintain 95% PCE after 500 h at 85 °C under continuous illumination, which would meet industrial standards for reliable solar cells.<sup>74</sup> The cathode luminescence measurements revealed that an appropriate addition of

RbI helped to avoid the unwanted yellow phase and distributed the PbI<sub>2</sub> phase and therefore increased the solar cell performance.<sup>75,76</sup> However, an addition of more than 10% RbI into the mixed cation perovskite resulted in a Rb-rich phase which was destructive to the cells. Although other alkali metals do not have suitable radii to form a stable perovskite structure, a small amount of lithium and sodium salts could also promote the crystallization process and enhance the solar cell performance.<sup>77,78</sup>

### 2D/3D mixed cation perovskites

As well as the regular 3D perovskite with the formula of ABX<sub>3</sub> with a small size cation,<sup>79</sup> use of the large size cation, especially the long chain alkylammonium cation, would form a low dimensional 2D perovskite with the formula of A<sub>2</sub>BX<sub>4</sub>. Usually the 3D perovskite exhibits a good photoabsorption coefficient, desirable band gap and long charge diffusion lengths, but the 3D perovskites application is significantly limited by their instability because of the ubiquitous water intercalation, ion migration, and thermal decomposition. In contrast, a 2D perovskite with a higher stability possesses poor electronic and optical properties with strongly bound excitons because of the poor transporting property of these long chain organic cations. To enhance the stability of the perovskite, 2D and 3D perovskite with different sized cations were combined to form multi-dimensional perovskites with balanced PV performance and stability.<sup>80</sup> In these 2D/3D mixed cation perovskites, the long chain cation in the 2D perovskites acts as moisture barriers whereas the 3D perovskites perform the optical-electric transfer. Unlike the MA, FA or Cs in a mixed cation perovskite of a suitable size to form periodic corner-shared perovskite alloy, the relatively larger size cation in a multi-dimensional perovskite will form a 2D/3D mixed perovskite. A typical formula for the 2D/3D mixed perovskite can be described as M<sub>2</sub>A<sub>n-1</sub>B<sub>n</sub>X<sub>3n+1</sub>. Usually M is a large cation such as phenylethylammonium (PEA),<sup>81,82</sup> poly(ethyleneimine) (PEI),<sup>83</sup> butylamine (BA),<sup>84,85</sup> cyclopropylamine (CA)<sup>86</sup> and A is MA, FA, or Cs, B is Pb or tin (Sn) and X is a halide anion such as I, Br or Cl and *n* is number of layers of metal-halide sheets. The 2D/3D mixed perovskites have also been successfully prepared using one-step deposition,<sup>81-85,87-93</sup> sequential deposition,<sup>94-96</sup> or 2D/3D perovskite post-treatment method.<sup>86,97-99</sup> A different method from having the larger

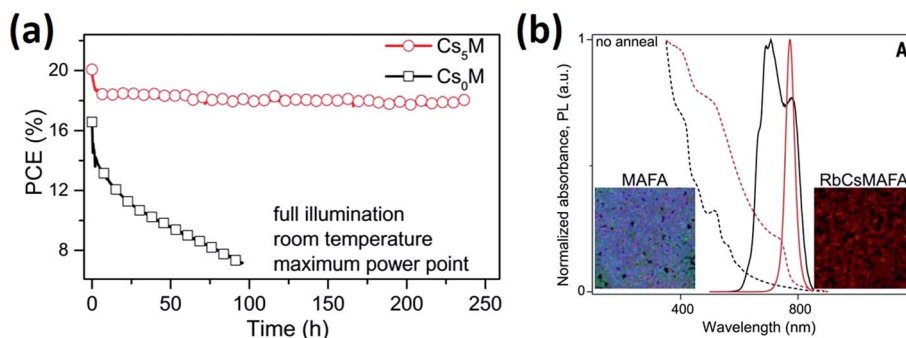


Fig. 6 (a) Solar cell performance and stability test of mixed cation perovskite (Cs/MA/FA) reproduced from ref. 69 with permission from the Royal Society of Chemistry. (b) The effect of incorporation of 5% Rb into mixed cation MA/FA perovskite solar cells. Reprinted with permission from ref. 74. Copyright © 2016, American Association for the Advancement of Science.

cation occupied in the A site is interlinkage which is another approach to design the 2D/3D structure. Li *et al.* prepared MAPbI<sub>3</sub> perovskite which was exposed to butylphosphonic acid 4-ammonium chloride (4-ABPACl) resulting in the incorporation of the perovskite into a mesoporous TiO<sub>2</sub> film with the hydrogen bonding of the –PO(OH)<sub>2</sub> and –NH<sub>3</sub><sup>+</sup> on the perovskite surface.<sup>87</sup> A uniform film and PCEs from 8.8% to 16.7% was achieved as well as good moisture resistance. In a recent work by Zhang *et al.*, formation of an *in situ* crosslinked 2D/3D NH<sub>3</sub>C<sub>4</sub>H<sub>9</sub>COO(CH<sub>2</sub>-NH<sub>3</sub>)<sub>n</sub>Pb<sub>n</sub>Br<sub>3n</sub> perovskite planar films with a controllable quantum confine were designed and prepared.<sup>100</sup> The crosslinkage was realized using the bifunctional amino acid with NH<sub>3</sub><sup>+</sup> and the COO<sup>-</sup> groups. The film showed a comparable PL quantum yield (PLQY) to perovskite quantum dots prepared using a classical hot injection technique.

The mixed 2D/3D perovskite (PEA)<sub>2</sub>(MA)<sub>2</sub>[Pb<sub>3</sub>I<sub>10</sub>] was prepared using a one-step method by simply spin coating the precursor mixture of (PEA)I, MAI and PbI<sub>2</sub>.<sup>81</sup> The 2D/3D structure of the layered perovskite (PEA)<sub>2</sub>(MA)<sub>2</sub>[Pb<sub>3</sub>I<sub>10</sub>] (PEA = C<sub>6</sub>H<sub>5</sub>(CH<sub>2</sub>)<sub>2</sub>NH<sub>3</sub><sup>+</sup>) shown in Fig. 7d exhibited an open-circuit voltage of 1.18 V and a PCE of 4.73%. The mixed perovskite (PEA)<sub>2</sub>(MA)<sub>2</sub>[Pb<sub>3</sub>I<sub>10</sub>] is much more resistant to moisture compared to the pure MAPbI<sub>3</sub> although the devices have a lower PCE than existing solar cells with 3D perovskite absorbers. Furthermore, the number of layers *n*, was explored by Cohen *et al.*<sup>82</sup> and Quan *et al.*<sup>88</sup> (Fig. 7e). The theoretical analysis and experimental results revealed that the devices based on (PEA)<sub>2</sub>(MA)<sub>n-1</sub>[Pb<sub>n</sub>I<sub>3n+1</sub>] with an *n* of 40 or 60 had both high PCE

and stability. Yao *et al.* used a polymeric ammonium PEI as an interlayer spacer formed mixed 2D/3D perovskite (PEI)<sub>2</sub>(MA)<sub>n-1</sub>Pb<sub>n</sub>I<sub>3n+1</sub> (*n* = 3, 5, 7).<sup>83</sup> The use of polymeric ammonium leads to the tight stacking of the separated Pb–I unit layers and thus promotes the charge transfer. A PCE of 8.77% was obtained on a 2.32 cm<sup>2</sup> size device. Cao *et al.* and Stoumpos *et al.* reported the one-step deposition of a (BA)<sub>2</sub>(MA)<sub>n-1</sub>Pb<sub>n</sub>I<sub>3n+1</sub> mixed perovskite with different layers (*n* = 1, 2, 3 and 4).<sup>84,85</sup> They found that the film grew along the [Pb<sub>n</sub>I<sub>3n+1</sub>] slabs perpendicular to the substrate leading to the formation of smooth and uniform perovskite films. The 2D/3D-based perovskite solar cells showed notable moisture resistance but also suffered from a low PCE of 4.02%. Also, combining the BA with inorganic cation Cs yielded a great stability even after exposure to 30% relative humidity (RH) or upon heating at 85 °C.<sup>93</sup> Later, Tsai *et al.* reported that by changing the film growth orientation by using the hot cast method, a preferential out-of-plane alignment film with a high film crystalline quality was formed (Fig. 8).<sup>89</sup> The charge transport was facilitated in this Ruddlesden–Popper perovskite solar cell to realize a record high PCE of 12.52% with a high tolerance to illumination and humidity.

The 2D/3D mixed perovskite of FA<sub>x</sub>PEA<sub>1-x</sub>PbI<sub>3</sub> can also be fabricated using a sequential deposition method as shown in Fig. 9a.<sup>101</sup> A high PCE of 17.7% was achieved because the PEA<sup>+</sup> cation promoted the perovskite phase and acted as passivation layer to resist moisture. The 2D/3D hybrid perovskite of (CA<sub>2</sub>PbI<sub>4</sub>/MAPbI<sub>x</sub>Cl<sub>3-x</sub>) exhibited significant humidity resistance up to 63 ± 5%.<sup>86</sup> Results showed that no degradation

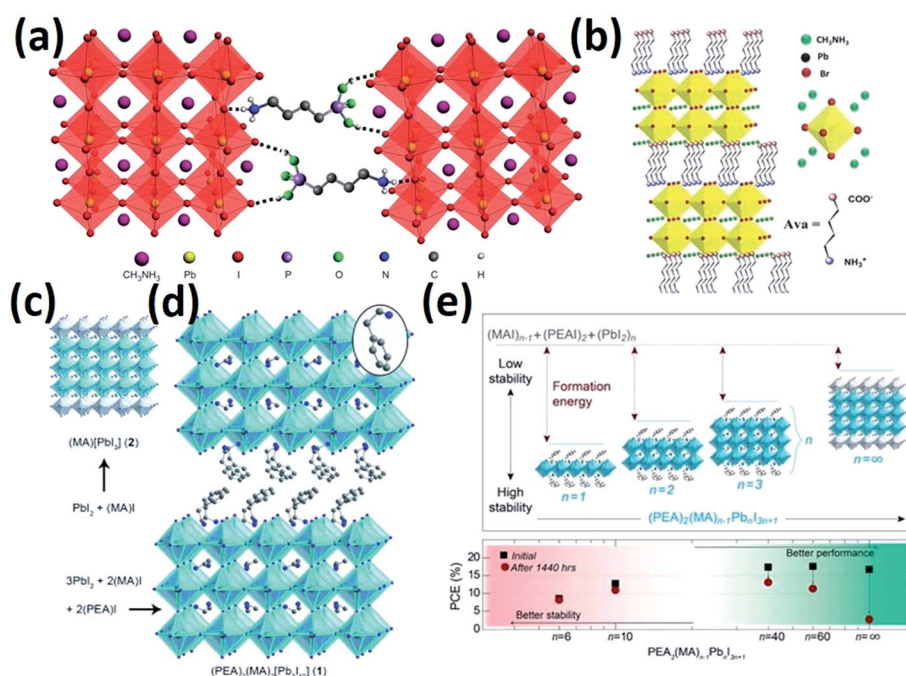


Fig. 7 (a) Schematic illustration of the crosslinking of CH<sub>3</sub>NH<sub>3</sub>PbI<sub>3</sub> structures by butylphosphonic acid 4-ammonium chloride (4-ABPACl). Reprinted with permission from ref. 87. Copyright © 2015, Rights Managed by Nature Publishing Group. (b) Crystal structure of crosslinked perovskite Ava(MAPbBr<sub>3</sub>)<sub>n</sub> (*n* = 2). Reprinted with permission from ref. 100. Copyright © 2016 WILEY-VCH Verlag GmbH & Co. KGaA, Weinheim. (c) and (d) Schematic illustration of 3D perovskite (MA)[PbI<sub>3</sub>] structure and mixed 2D/3D perovskite (PEA)<sub>2</sub>(MA)<sub>2</sub>[Pb<sub>3</sub>I<sub>10</sub>] structure. Reprinted with permission from ref. 81. Copyright © 2014 WILEY-VCH Verlag GmbH & Co. KGaA, Weinheim. (e) Perovskite structure and device performance of (PEA)<sub>2</sub>(MA)<sub>n-1</sub>Pb<sub>n</sub>I<sub>3n+1</sub> perovskites at different *n* values. Reprinted with permission from ref. 88. Copyright 2016 American Chemical Society.

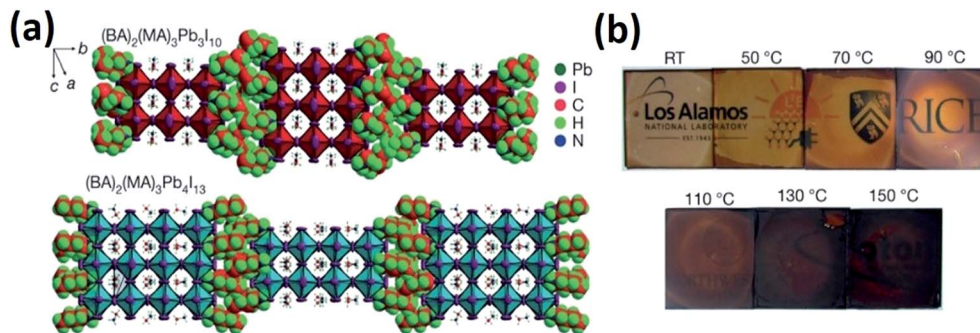


Fig. 8 (a) Illustration of the structure of the Ruddlesden–Popper  $(\text{BA})_2(\text{MA})_3\text{Pb}_3\text{I}_{10}$  and  $(\text{BA})_2(\text{MA})_3\text{Pb}_4\text{I}_{13}$  layered perovskites. (b) Photographs of  $(\text{BA})_2(\text{MA})_3\text{Pb}_4\text{I}_{13}$  thin films annealed at different temperatures. Reprinted with permission from ref. 89. Copyright© 2016, Rights Managed by Nature Publishing Group.

occurred in the 2D/3D perovskite after 40 days whereas the pure 3D perovskite decomposed completely under the same conditions after eight days. A controlled growth of a mixed cation perovskite  $(\text{IC}_2\text{H}_4\text{NH}_3)_2(\text{MA})_{n-1}\text{Pb}_n\text{I}_{3n+1}$  with a nanostructure was demonstrated by treating 2D perovskite  $(\text{IC}_2\text{H}_4\text{NH}_3)_2\text{Pb}_2\text{I}_4$  with MAI solution *via* sequential deposition (Fig. 9b).<sup>97</sup> Such perovskite films can be fabricated into a solar cell with PCE over 9%.

The larger organic cations such as  $\text{CF}_3\text{CH}_2\text{NH}_3$ ,<sup>102</sup>  $\text{NH}_3\text{-I}(\text{CH}_2)_8\text{NH}_3$ ,<sup>98</sup> and benzene-amine molecules<sup>99</sup> have also been considered for use as the surface passivation layer as well as the mixed 2D/3D perovskite. Wang *et al.* chose to use aniline, benzylamine, and phenethylamine as “moisture resistive” passivation molecules achieving PCEs above 19% and an excellent humidity stability of the benzylamine-characterized  $\text{FAPbI}_3$  after more than 2900 h exposed in air ( $50 \pm 5$  RH%).<sup>99</sup> Besides their application in solar cells, 2D/3D mixed perovskites are becoming one of most promising candidates for light-emitting diode (LED) device applications. Yuan *et al.* found that by partly replacing the MA cation with the larger PEA cation, the mixed perovskite  $\text{PEA}_2\text{MA}_{n-1}\text{Pb}_n\text{I}_{3n+1}$  showed a larger exciton binding energy, charge carrier concentrator behavior and an acceptable charge transport property, which facilitated the radiative recombination.<sup>90</sup> The device exhibited an external quantum PCE (EQE) of about 8.8% and radiance of  $80 \text{ W sr}^{-1} \text{ m}^{-2}$ . Byun *et al.* reported similar results from utilizing a  $\text{PEA}_2\text{MA}_{n-1}\text{Pb}_n\text{Br}_{3n+1}$  LED device.<sup>92</sup> An EQE of up to 11.7% with good stability was achieved by Wang *et al.* using a 2D/3D mixed perovskite.<sup>91</sup> In this work, a solution-processed perovskite with self-organized multiple quantum wells was obtained by mixing FAI and 1-naphthylmethylamine iodide to form a 2D/3D mixed perovskite. All these researches suggest that it is important to design a novel 2D/3D mixed perovskite with balanced electron transfer properties and stabilities.

#### Mixed cation to stabilize the Pb–Sn alloy metal halide perovskite

Because of the similar electronic structure and the similar ionic radii of Sn (1.35 Å) to Pb (1.49 Å), the Sn and Pb-free perovskites provide promising prospects with a toxicological advantage and a broader band gap tuning. Hao *et al.* reported

that the optical bandgap of  $\text{MASnI}_3$  was 1.3 eV resulting in an absorption set at 950 nm, which is ideal for solar cell applications.<sup>103</sup> Interestingly, the alloyed Pb/Sn MAI perovskite showed a bandgap not in the range between 1.55 eV and 1.35 eV but was narrower than 1.3 eV extending the absorption onset to the near-infrared.<sup>104–106</sup>

Based on the Shockley–Queisser theory, replacing 15% Pb by Sn in the perovskite can theoretically enhance the PCE from 27.9% to 30.4%.<sup>108</sup> However, the PCEs of solar cells based on the Sn perovskites were relatively low.<sup>103–105,109–114</sup> Other than the low PCE, another great problem that exists is that the favorable  $\text{Sn}^{2+}$  is prone to oxidize into the more stable  $\text{Sn}^{4+}$ , which will destroy the perovskite structure. Based on the spin polarized density functional theory calculations, Wang *et al.* found the Sn atom in  $\text{FASnI}_3$  were less likely to be oxidized to  $\text{Sn}^{4+}$  than in  $\text{MASnI}_3$  because of the stronger hydrogen bond in the  $\text{FASnI}_3$ .<sup>115</sup> Because of the FA oxidation shield effect, the MA or FA mixed cation perovskites with Sn substitution for Pb showed significant progress in the preparation of a stable Pb–Sn mixed perovskite. The  $(\text{FASnI}_3)_{1-x}(\text{MAPbI}_3)_x$  solar cell PEC has been greatly improved compared to the previously reported  $\text{CH}_3\text{NH}_3\text{Sn}_{1-x}\text{Pb}_x\text{I}_3$  perovskite.<sup>116–118</sup> The mixed FA/MA and Sn/Pb perovskite with inverted cell structure was prepared using  $\text{FASnI}_3$  and  $\text{MAPbI}_3$  precursor by Liao *et al.*<sup>119</sup> The indium tin oxide (ITO)/poly(3,4-ethylenedioxythiophene) polystyrene sulfonate (PEDOT:PSS)/ $(\text{FASnI}_3)_{0.6}(\text{MAPbI}_3)_{0.4}/\text{C}_{60}/\text{BCP}/\text{Ag}$  devices showed an increased PCE of 15.08% and a short-circuit current density of  $26.86 \text{ mA cm}^{-2}$  compared to previous studies. The Sn-based  $\text{MA}_{0.5}\text{FA}_{0.5}\text{Pb}_{0.75}\text{Sn}_{0.25}\text{I}_3$  perovskite solar cells can be fabricated *via* one-step method.<sup>120</sup> A PCE of 14.19% was achieved initially and was 94% after 30 days in an inert atmosphere and 80% after 12 days exposed to ambient atmosphere (30–40% RH). Once placed in tandem with  $\text{MAPbI}_3$  PSCs, it recorded a PCE of 19.08%. As shown in Fig. 10, Eperon *et al.* incorporated Sn into the mixed perovskite  $\text{FA}_{0.75}\text{Cs}_{0.25}\text{PbI}_3$  with a bandgap of 1.2 eV and 14.8% PCE.<sup>107</sup> In terms of stability, the  $\text{FA}_{0.75}\text{Cs}_{0.25}\text{Sn}_{0.5}\text{Pb}_{0.5}\text{I}_3$  films can be heated at 100 °C for four days and no moderating trend of PCE occurs.

In summary, the interest in mixed cation metal halide perovskite has demonstrated rapid progress in a short period of time to produce perovskite-based optoelectronic devices with

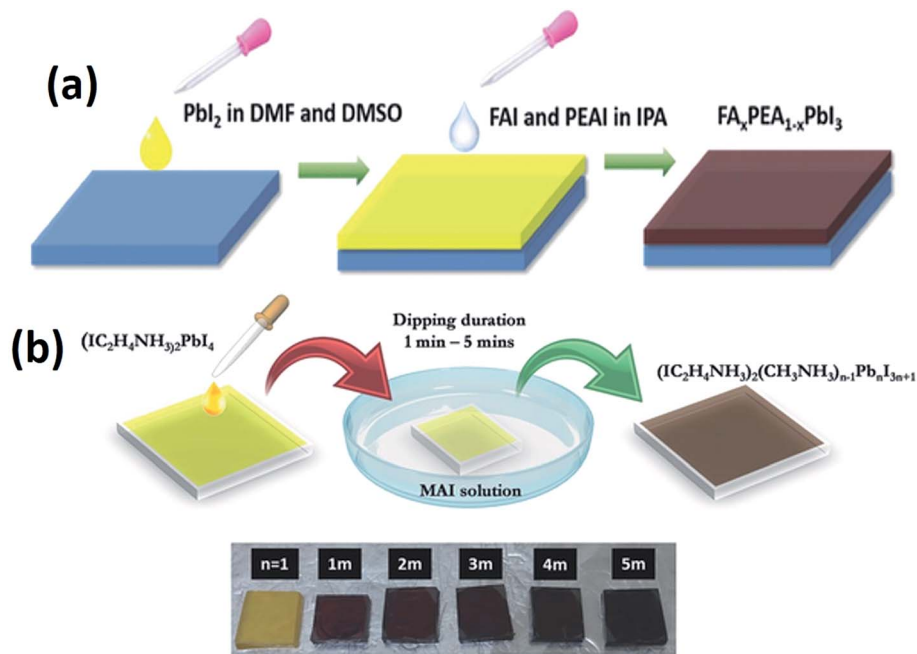


Fig. 9 (a) Schematic illustration of the preparation of  $\text{FA}_x\text{PEA}_{1-x}\text{PbI}_3$  films by sequential deposition. Reprinted with permission from ref. 101. Copyright© 2016 WILEY-VCH Verlag GmbH & Co. KGaA, Weinheim. (b) Controlled growth of mixed cation perovskites  $(\text{IC}_2\text{H}_4\text{NH}_3)_2(\text{MA})_{n-1}\text{Pb}_n\text{I}_{3n+1}$  using different dipping times. Reprinted with permission from ref. 97. Copyright© 2016 WILEY-VCH Verlag GmbH & Co. KGaA, Weinheim.

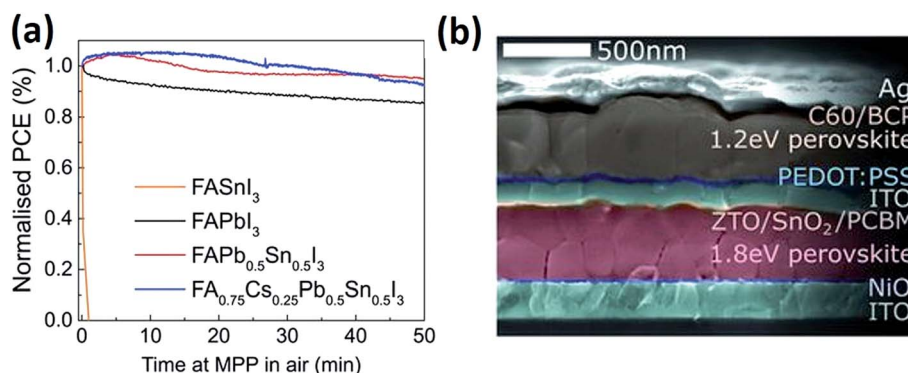


Fig. 10 (a) PCE as a function of time for  $\text{FASnI}_3$ ,  $\text{FAPbI}_3$ ,  $\text{FAPb}_{0.5}\text{Sn}_{0.5}\text{I}_3$  and  $\text{FA}_{0.75}\text{Cs}_{0.25}\text{Sn}_{0.5}\text{Pb}_{0.5}\text{I}_3$  in air under AM1.5G illumination. (b) Cross scanning electron microscopy of the two-terminal perovskite-perovskite tandem. Reprinted with permission from ref. 107. Copyright© 2016, American Association for the Advancement of Science.

enhanced performance and stability. The fast development can be ascribed to previous research efforts and results obtained using  $\text{MAPbI}_3$  perovskite. Further fundamental understanding of the mixed cation perovskite is expected to further improve perovskite solar cells to obtain PCEs greater than 22% and better stabilities. Because the phase purity of the mixed cation perovskite is so important and highly sensitive to deposition technique, it is essential to develop a scale-up method to deposit large sized, phase-pure, high quality mixed cation perovskite. Continued advances in mixed cation perovskite based optoelectronic devices will be based on a thorough understanding of the crystallization process and how different cations can affect the mixed cation perovskite. The strategy of

using mixed cation perovskites might also provide an opportunity to develop high performance, totally non-lead perovskite as demonstrated in current Pb-Sn alloyed perovskite. Other issues such as the phase separation in these mixed cation perovskites might be an issue for the long-term stability and the impact of different cation related stability issues should also be fully examined and understood.

## Acknowledgements

YZ acknowledges the support of the NSFC (Grant 51372151 and 21303103) and Huoyingdong Grant (151046).

## References

- NREL, [http://www.nrel.gov/ncpv/images/PCE\\_chart.jpg](http://www.nrel.gov/ncpv/images/PCE_chart.jpg).
- R. F. Service, *Science*, 2014, **344**, 458.
- B. Hailegnaw, S. Kirmayer, E. Edri, G. Hodes and D. Cahen, *J. Phys. Chem. Lett.*, 2015, **6**, 1543–1547.
- N.-G. Park, M. Grätzel, T. Miyasaka, K. Zhu and K. Emery, *Nat. Energy*, 2016, **1**, 16152.
- Y. Chen, M. He, J. Peng, Y. Sun and Z. Liang, *Adv. Sci.*, 2016, **3**, 1500392.
- D. Weber, *Z. Naturforsch., B: J. Chem. Sci.*, 1978, **33**, 862–865.
- O. Almora, I. Zarazua, E. Mas-Marza, I. Mora-Sero, J. Bisquert and G. Garcia-Belmonte, *J. Phys. Chem. Lett.*, 2015, **6**, 1645–1652.
- A. Kojima, K. Teshima, Y. Shirai and T. Miyasaka, *J. Am. Chem. Soc.*, 2009, **131**, 6050–6051.
- J.-H. Im, C.-R. Lee, J.-W. Lee, S.-W. Park and N.-G. Park, *Nanoscale*, 2011, **3**, 4088–4093.
- H.-S. Kim, C.-R. Lee, J.-H. Im, K.-B. Lee, T. Moehl, A. Marchioro, S.-J. Moon, R. Humphry-Baker, J.-H. Yum, J. E. Moser, M. Grätzel and N.-G. Park, *Sci. Rep.*, 2012, **2**, 1–7.
- M. M. Lee, J. Teuscher, T. Miyasaka, T. N. Murakami and H. J. Snaith, *Science*, 2012, **338**, 643–647.
- J. H. Heo, S. H. Im, J. H. Noh, T. N. Mandal, C.-S. Lim, J. A. Chang, Y. H. Lee, H.-j. Kim, A. Sarkar, K. Nazeeruddin, M. Grätzel and S. I. Seok, *Nat. Photonics*, 2013, **7**, 486–491.
- P. Gao, M. Grätzel and M. K. Nazeeruddin, *Energy Environ. Sci.*, 2014, **7**, 2448–2463.
- H. S. Jung and N.-G. Park, *Small*, 2014, **11**, 10–25.
- S. D. Stranks and H. J. Snaith, *Nat. Nanotechnol.*, 2015, **10**, 391–402.
- Y. Zhao and K. Zhu, *Chem. Soc. Rev.*, 2016, **45**, 655–689.
- Y. Zhao and K. Zhu, *J. Phys. Chem. Lett.*, 2014, **5**, 4175–4186.
- G. Niu, X. Guo and L. Wang, *J. Mater. Chem. A*, 2015, **3**, 8970–8980.
- I. Borriello, G. Cantele and D. Ninno, *Phys. Rev. B: Condens. Matter Mater. Phys.*, 2008, **77**, 235214.
- A. Amat, E. Mosconi, E. Ronca, C. Quarti, P. Umari, M. K. Nazeeruddin, M. Grätzel and F. De Angelis, *Nano Lett.*, 2014, **14**, 3608–3616.
- N. Pellet, P. Gao, G. Gregori, T. Y. Yang, M. K. Nazeeruddin, J. Maier and M. Grätzel, *Angew. Chem., Int. Ed. Engl.*, 2014, **53**, 3151–3157.
- M. Hu, L. Liu, A. Mei, Y. Yang, T. Liu and H. Han, *J. Mater. Chem. A*, 2014, **2**, 17115–17121.
- J. Liu, Y. Shirai, X. Yang, Y. Yue, W. Chen, Y. Wu, A. Islam and L. Han, *Adv. Mater.*, 2015, **27**, 4918–4923.
- J. Dai, Y. Fu, L. H. Manger, M. T. Rea, L. Hwang, R. H. Goldsmith and S. Jin, *J. Phys. Chem. Lett.*, 2016, 5036–5043.
- M. Bag, L. A. Renna, R. Y. Adhikari, S. Karak, F. Liu, P. M. Lahti, T. P. Russell, M. T. Tuominen and D. Venkataraman, *J. Am. Chem. Soc.*, 2015, **137**, 13130–13137.
- A. Binek, F. C. Hanusch, P. Docampo and T. Bein, *J. Phys. Chem. Lett.*, 2015, **6**, 1249–1253.
- F. Ji, L. Wang, S. Pang, P. Gao, H. Xu, G. Xie, J. Zhang and G. Cui, *J. Mater. Chem. A*, 2016, **4**, 14437–14443.
- G. E. Eperon, C. E. Beck and H. J. Snaith, *Mater. Horiz.*, 2016, **3**, 63–71.
- Y. Zhou, M. Yang, S. Pang, K. Zhu and N. P. Padture, *J. Am. Chem. Soc.*, 2016, **138**, 5535–5538.
- M. Salado, L. Calio, R. Berger, S. Kazim and S. Ahmad, *Phys. Chem. Chem. Phys.*, 2016, **18**, 27148–27157.
- X. Zheng, C. Wu, S. K. Jha, Z. Li, K. Zhu and S. Priya, *ACS Energy Lett.*, 2016, **1**, 1014–1020.
- W. S. Yang, J. H. Noh, N. J. Jeon, Y. C. Kim, S. Ryu, J. Seo and S. I. Seok, *Science*, 2015, **348**, 1234–1237.
- Q. Jiang, L. Zhang, H. Wang, X. Yang, J. Meng, H. Liu, Z. Yin, J. Wu, X. Zhang and J. You, *Nat. Energy*, 2016, **2**, 16177.
- N. J. Jeon, J. H. Noh, W. S. Yang, Y. C. Kim, S. Ryu, J. Seo and S. I. Seok, *Nature*, 2015, **517**, 476–480.
- Y. C. Kim, N. J. Jeon, J. H. Noh, W. S. Yang, J. Seo, J. S. Yun, A. Ho-Baillie, S. Huang, M. A. Green, J. Seidel, T. K. Ahn and S. I. Seok, *Adv. Energy Mater.*, 2016, **6**, 1502104.
- Z. Yang, C.-C. Chueh, P.-W. Liang, M. Crump, F. Lin, Z. Zhu and A. K. Y. Jen, *Nano Energy*, 2016, **22**, 328–337.
- D. Bi, W. Tress, M. I. Dar, P. Gao, J. Luo, C. Renevier, K. Schenk, A. Abate, F. Giordano, J.-P. Correa Baena, J.-D. Decoppet, S. M. Zakeeruddin, M. K. Nazeeruddin, M. Grätzel and A. Hagfeldt, *Sci. Adv.*, 2016, **2**, 1501170.
- D. Bi, C. Yi, J. Luo, J.-D. Decoppet, F. Zhang, S. M. Zakeeruddin, X. Li, A. Hagfeldt and M. Grätzel, *Nat. Energy*, 2016, **1**, 16142.
- T. Jesper Jacobsson, J.-P. Correa-Baena, M. Pazoki, M. Saliba, K. Schenk, M. Grätzel and A. Hagfeldt, *Energy Environ. Sci.*, 2016, **9**, 1706–1724.
- P. Gratia, G. Grancini, J.-N. Audinot, X. Jeanbourquin, E. Mosconi, I. Zimmermann, D. Dowsett, Y. Lee, M. Grätzel, F. De Angelis, K. Sivula, T. Wirtz and M. K. Nazeeruddin, *J. Am. Chem. Soc.*, 2016, **138**, 15821–15824.
- W. Tress, J. P. Correa Baena, M. Saliba, A. Abate and M. Graetzel, *Adv. Energy Mater.*, 2016, **6**, 1600396.
- J. Zhang, Y. Hua, B. Xu, L. Yang, P. Liu, M. B. Johansson, N. Vlachopoulos, L. Kloo, G. Boschloo, E. M. J. Johansson, L. Sun and A. Hagfeldt, *Adv. Energy Mater.*, 2016, **6**, 1601062.
- J. P. C. Baena, L. Steier, W. Tress, M. Saliba, S. Neutzner, T. Matsui, F. Giordano, T. J. Jacobsson, A. R. S. Kandada and S. M. Zakeeruddin, *Energy Environ. Sci.*, 2015, **8**, 2928–2934.
- A. Guerrero, G. Garcia-Belmonte, I. Mora-Sero, J. Bisquert, Y. S. Kang, T. J. Jacobsson, J.-P. Correa-Baena and A. Hagfeldt, *J. Phys. Chem. C*, 2016, **120**, 8023–8032.
- Y. H. Lee, J. Luo, M.-K. Son, P. Gao, K. T. Cho, J. Seo, S. M. Zakeeruddin, M. Grätzel and M. K. Nazeeruddin, *Adv. Mater.*, 2016, **28**, 3966–3972.
- J. Zhang, B. Xu, M. B. Johansson, M. Hadadian, J. P. Correa Baena, P. Liu, Y. Hua, N. Vlachopoulos, E. M. J. Johansson,

- G. Boschloo, L. Sun and A. Hagfeldt, *Adv. Energy Mater.*, 2016, **6**, 1502536.
- 47 D. Bi, B. Xu, P. Gao, L. Sun, M. Grätzel and A. Hagfeldt, *Nano Energy*, 2016, **23**, 138–144.
- 48 M. Cheng, C. Chen, K. Aitola, F. Zhang, Y. Hua, G. Boschloo, L. Kloo and L. Sun, *Chem. Mater.*, 2016, **28**, 8631–8639.
- 49 I. Cho, N. J. Jeon, O. K. Kwon, D. W. Kim, E. H. Jung, J. H. Noh, J. Seo, S. I. Seok and S. Y. Park, *Chem. Sci.*, 2017, **8**, 734–741.
- 50 B. Xu, D. Bi, Y. Hua, P. Liu, M. Cheng, M. Grätzel, L. Kloo, A. Hagfeldt and L. Sun, *Energy Environ. Sci.*, 2016, **9**, 873–877.
- 51 M. Saliba, S. Orlandi, T. Matsui, S. Aghazada, M. Cavazzini, J.-P. Correa-Baena, P. Gao, R. Scopelliti, E. Mosconi, K.-H. Dahmen, F. De Angelis, A. Abate, A. Hagfeldt, G. Pozzi, M. Graetzel and M. K. Nazeeruddin, *Nat. Energy*, 2016, **1**, 15017.
- 52 Y. Wu, X. Yang, W. Chen, Y. Yue, M. Cai, F. Xie, E. Bi, A. Islam and L. Han, *Nat. Energy*, 2016, **1**, 16148.
- 53 L.-C. Chen, Z.-L. Tseng and J.-K. Huang, *Nanomaterials*, 2016, **6**, 183.
- 54 L.-C. Chen, J.-R. Wu, Z.-L. Tseng, C.-C. Chen, H. S. Chang, J.-K. Huang, K.-L. Lee and H.-M. Cheng, *Materials*, 2016, **9**, 747.
- 55 F. H. Isikgor, B. Li, H. Zhu, Q. Xu and J. Ouyang, *J. Mater. Chem. A*, 2016, **4**, 12543–12553.
- 56 G. Li, T. Zhang, N. Guo, F. Xu, X. Qian and Y. Zhao, *Angew. Chem., Int. Ed.*, 2016, **55**, 13460–13464.
- 57 Y. Reyna, M. Salado, S. Kazim, A. Pérez-Tomas, S. Ahmad and M. Lira-Cantu, *Nano Energy*, 2016, **30**, 570–579.
- 58 K. Sveinbjornsson, K. Aitola, J. Zhang, M. B. Johansson, X. Zhang, J.-P. Correa-Baena, A. Hagfeldt, G. Boschloo and E. M. J. Johansson, *J. Mater. Chem. A*, 2016, **4**, 16536–16545.
- 59 B. Conings, J. Drijkoningen, N. Gauquelin, A. Babayigit, J. D'Haen, L. D'Olieslaeger, A. Ethirajan, J. Verbeeck, J. Manca, E. Mosconi, F. D. Angelis and H.-G. Boyen, *Adv. Energy Mater.*, 2015, **5**, 1500477.
- 60 G. E. Eperon, G. M. Paterno, R. J. Sutton, A. Zampetti, A. A. Haghighirad, F. Cacialli and H. J. Snaith, *J. Mater. Chem. A*, 2015, **3**, 19688–19695.
- 61 Z. Li, M. Yang, J.-S. Park, S.-H. Wei, J. J. Berry and K. Zhu, *Chem. Mater.*, 2016, **28**, 284–292.
- 62 R. E. Beal, D. J. Slotcavage, T. Leijtens, A. R. Bowering, R. A. Belisle, W. H. Nguyen, G. F. Burkhard, E. T. Hoke and M. D. McGehee, *J. Phys. Chem. Lett.*, 2016, **7**, 746–751.
- 63 J. W. Lee, D. H. Kim, H. S. Kim, S. W. Seo, S. M. Cho and N. G. Park, *Adv. Energy Mater.*, 2015, **5**, 1501310.
- 64 C. Yi, J. Luo, S. Meloni, A. Boziki, N. Ashari-Astani, C. Grätzel, S. M. Zakeeruddin, U. Röthlisberger and M. Grätzel, *Energy Environ. Sci.*, 2016, **9**, 656–662.
- 65 W. Rehman, D. P. McMeekin, J. B. Patel, R. L. Milot, M. B. Johnston, H. J. Snaith and L. M. Herz, *Energy Environ. Sci.*, 2017, **10**, 361–369.
- 66 D. P. McMeekin, G. Sadoughi, W. Rehman, G. E. Eperon, M. Saliba, M. T. Hörantner, A. Haghighirad, N. Sakai, L. Korte and B. Rech, *Science*, 2016, **351**, 151–155.
- 67 Z. Wang, D. P. McMeekin, N. Sakai, S. van Reenen, K. Wojciechowski, J. B. Patel, M. B. Johnston and H. J. Snaith, *Adv. Mater.*, 2016, **4**, 186.
- 68 H. Choi, J. Jeong, H.-B. Kim, S. Kim, B. Walker, G.-H. Kim and J. Y. Kim, *Nano Energy*, 2014, **7**, 80–85.
- 69 M. Saliba, T. Matsui, J.-Y. Seo, K. Domanski, J.-P. Correa-Baena, M. K. Nazeeruddin, S. M. Zakeeruddin, W. Tress, A. Abate and A. Hagfeldt, *Energy Environ. Sci.*, 2016, **9**, 1989–1997.
- 70 T. Matsui, J.-Y. Seo, M. Saliba, S. M. Zakeeruddin and M. Grätzel, *Adv. Mater.*, 2017, 1606258.
- 71 B. Conings, A. Babayigit, M. T. Klug, S. Bai, N. Gauquelin, N. Sakai, J. T.-W. Wang, J. Verbeeck, H.-G. Boyen and H. J. Snaith, *Adv. Mater.*, 2016, **28**, 10701–10709.
- 72 G. Kieslich, S. Sun and A. K. Cheetham, *Chem. Sci.*, 2014, **5**, 4712–4715.
- 73 M. R. Filip, G. E. Eperon, H. J. Snaith and F. Giustino, *Nat. Commun.*, 2014, **5**, 5757.
- 74 M. Saliba, T. Matsui, K. Domanski, J.-Y. Seo, A. Ummadisingu, S. M. Zakeeruddin, J.-P. Correa-Baena, W. R. Tress, A. Abate, A. Hagfeldt and M. Grätzel, *Science*, 2016, **354**, 206–209.
- 75 T. Duong, H. K. Mulmudi, H. Shen, Y. Wu, C. Barugkin, Y. O. Mayon, H. T. Nguyen, D. Macdonald, J. Peng, M. Lockrey, W. Li, Y.-B. Cheng, T. P. White, K. Weber and K. Catchpole, *Nano Energy*, 2016, **30**, 330–340.
- 76 O. A. Syzgantseva, M. Saliba, M. Grätzel and U. Rothlisberger, *J. Phys. Chem. Lett.*, 2017, **8**, 1191–1196.
- 77 J. Chang, Z. Lin, H. Zhu, F. H. Isikgor, Q.-H. Xu, C. Zhang, Y. Hao and J. Ouyang, *J. Mater. Chem. A*, 2016, **4**, 16546–16552.
- 78 K. M. Boopathi, R. Mohan, T.-Y. Huang, W. Budiawan, M.-Y. Lin, C.-H. Lee, K.-C. Ho and C.-W. Chu, *J. Mater. Chem. A*, 2016, **4**, 1591–1597.
- 79 C. C. Stoumpos, C. D. Malliakas and M. G. Kanatzidis, *Inorg. Chem.*, 2013, **52**, 9019–9038.
- 80 T. M. Koh, K. Thirumal, H. S. Soo and N. Mathews, *ChemSusChem*, 2016, **9**, 2541–2558.
- 81 I. C. Smith, E. T. Hoke, D. Solis-Ibarra, M. D. McGehee and H. I. Karunadasa, *Angew. Chem., Int. Ed.*, 2014, **53**, 11232–11235.
- 82 B.-E. Cohen, M. Wierzbowska and L. Etgar, *Adv. Funct. Mater.*, 2017, **27**, 1604733.
- 83 K. Yao, X. Wang, Y.-x. Xu, F. Li and L. Zhou, *Chem. Mater.*, 2016, **28**, 3131–3138.
- 84 D. H. Cao, C. C. Stoumpos, O. K. Farha, J. T. Hupp and M. G. Kanatzidis, *J. Am. Chem. Soc.*, 2015, **137**, 7843–7850.
- 85 C. C. Stoumpos, D. H. Cao, D. J. Clark, J. Young, J. M. Rondinelli, J. I. Jang, J. T. Hupp and M. G. Kanatzidis, *Chem. Mater.*, 2016, **28**, 2852–2867.
- 86 C. Ma, C. Leng, Y. Ji, X. Wei, K. Sun, L. Tang, J. Yang, W. Luo, C. Li, Y. Deng, S. Feng, J. Shen, S. Lu, C. Du and H. Shi, *Nanoscale*, 2016, **8**, 18309–18314.
- 87 X. Li, M. Ibrahim Dar, C. Yi, J. Luo, M. Tschumi, S. M. Zakeeruddin, M. K. Nazeeruddin, H. Han and M. Grätzel, *Nat. Chem.*, 2015, **7**, 703–711.

- 88 L. N. Quan, M. Yuan, R. Comin, O. Voznyy, E. M. Beauregard, S. Hoogland, A. Buin, A. R. Kirmani, K. Zhao, A. Amassian, D. H. Kim and E. H. Sargent, *J. Am. Chem. Soc.*, 2016, **138**, 2649–2655.
- 89 H. Tsai, W. Nie, J.-C. Blancon, C. C. Stoumpos, R. Asadpour, B. Harutyunyan, A. J. Neukirch, R. Verduzco, J. J. Crochet, S. Tretiak, L. Pedesseau, J. Even, M. A. Alam, G. Gupta, J. Lou, P. M. Ajayan, M. J. Bedzyk, M. G. Kanatzidis and A. D. Mohite, *Nature*, 2016, **536**, 312–316.
- 90 M. Yuan, L. N. Quan, R. Comin, G. Walters, R. Sabatini, O. Voznyy, S. Hoogland, Y. Zhao, E. M. Beauregard, P. Kanjanaboos, Z. Lu, D. H. Kim and E. H. Sargent, *Nat. Nanotechnol.*, 2016, **11**, 872–877.
- 91 N. Wang, L. Cheng, R. Ge, S. Zhang, Y. Miao, W. Zou, C. Yi, Y. Sun, Y. Cao, R. Yang, Y. Wei, Q. Guo, Y. Ke, M. Yu, Y. Jin, Y. Liu, Q. Ding, D. Di, L. Yang, G. Xing, H. Tian, C. Jin, F. Gao, R. H. Friend, J. Wang and W. Huang, *Nat. Photonics*, 2016, **10**, 699–704.
- 92 J. Byun, H. Cho, C. Wolf, M. Jang, A. Sadhanala, R. H. Friend, H. Yang and T.-W. Lee, *Adv. Mater.*, 2016, **28**, 7515–7520.
- 93 J.-F. Liao, H.-S. Rao, B.-X. Chen, D.-B. Kuang and C.-Y. Su, *J. Mater. Chem. A*, 2017, **5**, 2066–2072.
- 94 K. Yao, X. Wang, Y.-x. Xu and F. Li, *Nano Energy*, 2015, **18**, 165–175.
- 95 N. Li, Z. Zhu, C.-C. Chueh, H. Liu, B. Peng, A. Petrone, X. Li, L. Wang and A. K. Y. Jen, *Adv. Energy Mater.*, 2016, **7**, 1601307.
- 96 K. Yao, X. Wang, F. Li and L. Zhou, *Chem. Commun.*, 2015, **51**, 15430–15433.
- 97 T. M. Koh, V. Shanmugam, J. Schlipf, L. Oesinghaus, P. Müller-Buschbaum, N. Ramakrishnan, V. Swamy, N. Mathews, P. P. Boix and S. G. Mhaisalkar, *Adv. Mater.*, 2016, **28**, 3653–3661.
- 98 T. Zhao, C.-C. Chueh, Q. Chen, A. Rajagopal and A. K. Y. Jen, *ACS Energy Lett.*, 2016, **1**, 757–763.
- 99 F. Wang, W. Geng, Y. Zhou, H.-H. Fang, C.-J. Tong, M. A. Loi, L.-M. Liu and N. Zhao, *Adv. Mater.*, 2016, **28**, 9986–9992.
- 100 T. Zhang, L. Xie, L. Chen, N. Guo, G. Li, Z. Tian, B. Mao and Y. Zhao, *Adv. Funct. Mater.*, 2017, **27**, 1603568.
- 101 N. Li, Z. Zhu, C.-C. Chueh, H. Liu, B. Peng, A. Petrone, X. Li, L. Wang and A. K. Y. Jen, *Adv. Energy Mater.*, 2017, **7**, 1601307.
- 102 D. Bi, P. Gao, R. Scopelliti, E. Oveisi, J. Luo, M. Grätzel, A. Hagfeldt and M. K. Nazeeruddin, *Adv. Mater.*, 2016, **28**, 2910–2915.
- 103 F. Hao, C. C. Stoumpos, D. H. Cao, R. P. H. Chang and M. G. Kanatzidis, *Nat. Photonics*, 2014, **8**, 489–494.
- 104 F. Hao, C. C. Stoumpos, R. P. H. Chang and M. G. Kanatzidis, *J. Am. Chem. Soc.*, 2014, **136**, 8094–8099.
- 105 Y. Ogomi, A. Morita, S. Tsukamoto, T. Saitho, N. Fujikawa, Q. Shen, T. Toyoda, K. Yoshino, S. S. Pandey, T. Ma and S. Hayase, *J. Phys. Chem. Lett.*, 2014, **5**, 1004–1011.
- 106 J. Im, C. C. Stoumpos, H. Jin, A. J. Freeman and M. G. Kanatzidis, *J. Phys. Chem. Lett.*, 2015, **6**, 3503–3509.
- 107 G. E. Eperon, T. Leijtens, K. A. Bush, R. Prasanna, M. D. McGehee and H. J. Snaith, *et. al.*, *Science*, 2016, **354**, 861–865.
- 108 M. Anaya, J. P. Correa-Baena, G. Lozano, M. Saliba, P. Anguita, B. Roose, A. Abate, U. Steiner, M. Gratzel, M. E. Calvo, A. Hagfeldt and H. Miguez, *J. Mater. Chem. A*, 2016, **4**, 11214–11221.
- 109 N. K. Noel, S. D. Stranks, A. Abate, C. Wehrenfennig, S. Guarnera, A.-A. Haghighirad, A. Sadhanala, G. E. Eperon, S. K. Pathak, M. B. Johnston, A. Petrozza, L. M. Herz and H. J. Snaith, *Energy Environ. Sci.*, 2014, **7**, 3061–3068.
- 110 F. Zuo, S. T. Williams, P.-W. Liang, C.-C. Chueh, C.-Y. Liao and A. K. Y. Jen, *Adv. Mater.*, 2014, **26**, 6454–6460.
- 111 T. M. Koh, T. Krishnamoorthy, N. Yantara, C. Shi, W. L. Leong, P. P. Boix, A. C. Grimsdale, S. G. Mhaisalkar and N. Mathews, *J. Mater. Chem. A*, 2015, **3**, 14996–15000.
- 112 S. J. Lee, S. S. Shin, Y. C. Kim, D. Kim, T. K. Ahn, J. H. Noh, J. Seo and S. I. Seok, *J. Am. Chem. Soc.*, 2016, **138**, 3974–3977.
- 113 W. Ke, C. C. Stoumpos, J. L. Logsdon, M. R. Wasielewski, Y. Yan, G. Fang and M. G. Kanatzidis, *J. Am. Chem. Soc.*, 2016, **138**, 14998–15003.
- 114 C.-M. Tsai, H.-P. Wu, S.-T. Chang, C.-F. Huang, C.-H. Wang, S. Narra, Y.-W. Yang, C.-L. Wang, C.-H. Hung and E. W.-G. Diau, *ACS Energy Lett.*, 2016, **1**, 1086–1093.
- 115 F. Wang, J. Ma, F. Xie, L. Li, J. Chen, J. Fan and N. Zhao, *Adv. Funct. Mater.*, 2016, **26**, 3417–3423.
- 116 B. Zhao, M. Abdi-Jalebi, M. Tabachnyk, H. Glass, V. S. Kamboj, W. A. Nie, J. Pearson, Y. Puttisong, K. C. Gödel, H. E. Beere, D. A. Ritchie, A. D. Mohite, S. E. Dutton, R. H. Friend and A. Sadhanala, *Adv. Mater.*, 2017, **29**, 1604744.
- 117 L. Zhu, B. Yuh, S. Schoen, X. Li, M. Aldighaithir, B. J. Richardson, A. Alamer and Q. Yu, *Nanoscale*, 2016, **8**, 7621–7630.
- 118 Z. Yang, A. Rajagopal, S. B. Jo, C.-C. Chueh, S. Williams, C.-C. Huang, J. K. Katahara, H. W. Hillhouse and A. K. Y. Jen, *Nano Lett.*, 2016, **16**, 7739–7747.
- 119 W. Liao, D. Zhao, Y. Yu, N. Shrestha, K. Ghimire, C. R. Grice, C. Wang, Y. Xiao, A. J. Cimaroli, R. J. Ellingson, N. J. Podraza, K. Zhu, R.-G. Xiong and Y. Yan, *J. Am. Chem. Soc.*, 2016, **138**, 12360–12363.
- 120 Z. Yang, A. Rajagopal, C.-C. Chueh, S. B. Jo, B. Liu, T. Zhao and A. K. Y. Jen, *Adv. Mater.*, 2016, **28**, 8990–8997.